Available online at www.sciencedirect.com
ScienceDirect
Trans. Nonferrous Met. Soc. China 20(2010) 432−436
Transactions of Nonferrous Metals Society of China
www.tnmsc.cn

Sol-gel synthesis and photoluminescence of $LaPO_4$:Eu^{3+} nanorods

GAO Rui(高 锐)[1], QIAN Dong(钱 东)[1], LI Wei(李 卫)[1, 2]

1. School of Chemistry and Chemical Engineering, Central South University, Changsha 410083, China;
2. State Key Laboratory of Powder Metallurgy, Central South University, Changsha 410083, China

Received 18 September 2009; accepted 14 January 2010

Abstract: Monoclinic $LaPO_4$ nanostructures with uniform rod shape have been successfully synthesized by a simple sol-gel method. The procedure involves formation of homogeneous, transparent, metal-citrate-EDTA gel precursors, followed by calcination to promote thermal decomposition of the gel precursors to yield the $LaPO_4$ nanoparticles. Their morphologies and structures were characterized by XRD, TEM, TG-DSC and HRTEM. The results indicate that single monoclinic phase $LaPO_4$ nanorods are readily obtained at 800 ℃ within 3 h. Furthermore, photoluminescence (PL) characterization of the Eu^{3+}-doped $LaPO_4$ nanocrystals was carried out. The effects of calcination temperatures and Eu^{3+} doping content on the PL properties were elaborated in detail. Room-temperature photoluminescence (PL) characterization reveals that the optical brightness as well as the intensity ratio of $^5D_0$-$^7F_1$ to $^5D_0$-$^7F_2$ is highly dependent on the calcination temperature, and the $Eu_{0.05}La_{0.95}PO_4$ nanophosphor shows the relatively promising PL performance with the most intense emission.

Key words: $LaPO_4$; Eu doping; sol-gel; nanorods; photoluminescence

1 Introduction

The useful applications of rare earth element compounds, especially lanthanide phosphate doped inorganic materials, have been touched upon broadly. Over the past a few years, they have been applied in many fields, such as optical display panels, cathode ray tubes, optoelectronic, sensitive device, nanoscale electronic and plasma display panels[1−4] due to their special chemical and physical properties.

Various solution-phase routes, including combustion[5], sol-gel[6−7], precipitation[8], water-oil microemulsion[9], polyol-mediated process[10], ultrasonification[11], hydrothermal[12−14], and mechanochemical method[15], have been tried to lower the reaction temperature and obtain high-quality $LaPO_4$-based nanoparticles. However, the simple and mass fabrication of $LaPO_4$ nanocrystals with narrow grain size distribution and uniform morphology still remains a challenge. It appears that the best solution both to control powder morphology and to produce low cost thin films is the use of soft chemistry routes, in particular the sol-gel process since the intimate mixing of components ensure homogeneity of the final product. The sol-gel methods also have some obvious advantages compared with other ways, such as low processing temperature, easy coating of large surfaces, possible formation of porous films and homogeneous multicomponent oxide films as well as simple and cheap experimental setups. This sol-gel process is widely used for oxides materials which are the mostly used materials in phosphor technology by far.

In this regard, many research efforts have been taken on the upgrade of luminescence[16] of lanthanide compounds and control of the morphologies[17−18]. Nanoscale $LaPO_4$ with small grain shape has been synthesized via sol-gel reaction by RAJESH et al[7], and the yield of product is 85%. This work mainly worked on the elevation of the emitting wavelength and intensity by synthesis of $LaPO_4$ nannorods which could be used in biomedical image as quantum dots[19]. We adopted a simple sol-gel way to prepare $LaPO_4$ with good morphologies and fine crystal structures; and its emission and intensity of luminescence were also studied.

Foundation item: Project(50972166) supported by the National Natural Science Foundation of China; Project supported by the Scientific Research Foundation for the Returned Overseas Chinese Scholars, State Education Ministry, China
Corresponding author: LI Wei; Tel: +86-731-88830768; E-mail: csu973@163.com
DOI: 10.1016/S1003-6326(09)60158-8

2 Experimental

2.1 Synthesis of $LaPO_4$

All the chemical reagents were analytically pure and used without further purification. In a typical procedure, 0.01 mol of ethylenediamine tetraacetic acid (EDTA) was dissolved in 1 mol/L ammonia solution, then 0.45 mol/L $La(NO_3)_3$ aqueous solution was added dropwise to 1 mol/L CA solution under vigorous stirring. After that, this mixed solution and 0.5 mol/L of $NH_4H_2PO_4$ aqueous solution were added dropwise to the already dissolved EDTA solution by fiercely stirring. The pH of the solution under these steps was kept at 10−11 by using the ammonia solution as necessary. Then, the mixed solution was heated at 90 ℃ in a water bath with strong stirring as far as a transparent mixed sol was consequently obtained. The obtained sol was then transferred into an oven at 120 ℃ for 1 h to produce a viscous and black gel. The acquired gel subsequently was calcined for 3 h in muffle at 800 ℃ to fabricate the final white $LaPO_4$ nanoparticle.

2.2 Synthesis of Eu^{3+}-doped $LaPO_4$

The synthesis of the Eu^{3+}-doped $LaPO_4$ nanoparticles was the same with above described methods except for the addition of a certain amount of $Eu(NO_3)_3$ which was gained by Eu_2O_3 dissolved in 1 mol/L nitric acid after dropping of the $La(NO_3)_3$ aqueous solution. And the molar fractions of Eu^{3+} in the obtained products were 1%, 5% and 10%, respectively.

2.3 Sample characterization

Phase structures of the as-prepared samples were identified with X-ray powder diffraction (XRD) taken on a Rigaku-D-Max rA 12 kW diffractometer with Cu K_α radiation (λ=1.540 56 Å) at an operation voltage and current of 40 kV and 300 mA, respectively. The morphologies and sizes of the final products were characterized with a Hitachi H−800 transmission electron microscope (TEM) as well as high-resolution transmission electron microscope (HRTEM, JEOL−3010). The thermal decomposition behavior of the citrate gel precursors was examined by a thermogravimetric analyzer (TGA, Perkin-Elmer, TAC7/DX) using air as the working gas. For DSC measurements, the samples were heated from room temperature to 950 ℃ at a heating rate of 15 K/min. α-Al_2O_3 was used as the reference material, and the samples were run in open platinum pans. The PL measurements were carried out by using a Hitachi F−4500 fluorescence spectrophotometer. The excitation and emission spectra were corrected for the beam intensity variation in the Xe light source used. For comparison, all excitation and emission spectra were measured at room temperature with the same instrumental parameters.

3 Results and discussion

3.1 Thermal analysis

To clarify the chemical reaction during the thermal decomposition of the precursors, the thermal decomposition procedure of the obtained La-P-Citrate-EDTA gel precursors was studied by thermogravimetric/differential scanning calorimetry (TG-DSC) and the results are shown in Fig.1. From the TG curve, in the temperature range from ambient temperature to 600 ℃, three mass loss regions occur at 28−200 ℃(about 4.20%), 200−350 ℃ (about 27.20%), and 350−600 ℃ (about 41.05%). No significant mass loss can be observed from 600 to 800 ℃. Correspondingly, five discrete regions of thermal decomposition can be found in the DSC curve. The first endothermic peak centered at 99 ℃ corresponds to the elimination of water. Due to the elimination of molecule water, the second endothermic peak centered at 236 ℃ appears. The following two exothermic peaks centered at around 342 ℃ and 438 ℃ can also be ascribed to the combustion of the nitrate and the organic phases (EDTA). Subsequently, the third exothermic peak centered at 651 ℃ can be attributed to the elimination of the remaining organic materials (carbon and any other organic compounds) accompanied by the crystallization of the $LaPO_4$ inorganic phase[6, 20].

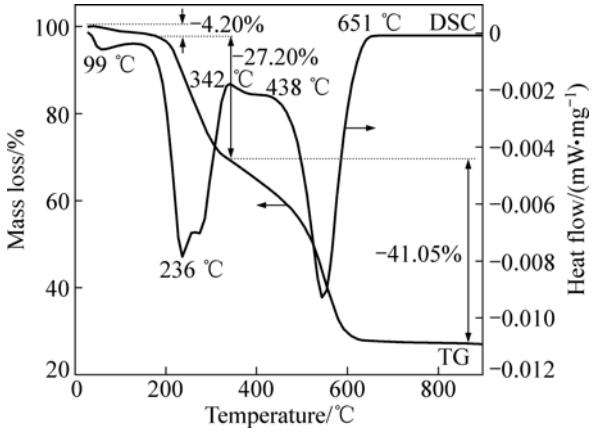

Fig.1 TG-DSC curves of as-synthesized metal-citrate-EDTA precursors

3.2 XRD analysis

The XRD patterns of the as-obtained samples are shown in Fig.2. It can be observed that the samples synthesized by sol-gel method at different temperatures crystallize in the monazite $LaPO_4$[8] (JCPDS 35-0731). From the main planes of $(\bar{1}11)$, (200), (120), $(\bar{1}12)$

and $(\bar{3}01)$, we can conclude that the intensity of the diffraction peaks gradually increases with the increase of temperature, revealing that the particle size increases and crystallinity increases with temperature. Moreover, no diffraction peaks for other phases are found in the XRD patterns.

Fig.3 shows the XRD patterns of the as-synthesized $Eu_xLa_{1-x}PO_4$ (x=0−0.1) with varying Eu^{3+} doping concentration compared with the $LaPO_4$ sample. It is also found that all the diffraction peaks can be readily indexed into pure-phase $LaPO_4$. Apparently, after doping with Eu^{3+}, the obtained samples remain a single phase, which indicates that Eu^{3+} can be effectively doped into the $LaPO_4$ lattice. And from the diffraction peaks of the main planes, we can also clearly see that the 5% Eu^{3+} doped sample has the best crystallinity.

3.3 TEM analysis

Fig.4 shows the TEM and HRTEM images of uniform $LaPO_4$ and $Eu_{0.05}La_{0.95}PO_4$ nanoparticles. It can be found from Fig.4(a) that the average length of $Eu_{0.05}La_{0.95}PO_4$ nanorods is around 60 nm. Fig.4(b) demonstrates the pure $LaPO_4$ nanorods sample is about 50 nm in length. From the HRTEM image of the sample shown in Fig.4(c), it can be seen that the as-synthesized $Eu_{0.05}La_{0.95}PO_4$ primary nanoparticles are well crystallized and ordered in crystallography.

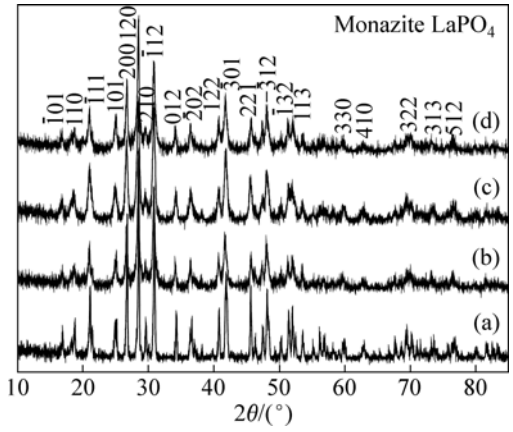

Fig.2 XRD patterns of as-prepared $LaPO_4$ samples synthesized at different temperatures: (a) 1 000 ℃; (b) 900 ℃; (c) 800 ℃; (d) 700 ℃

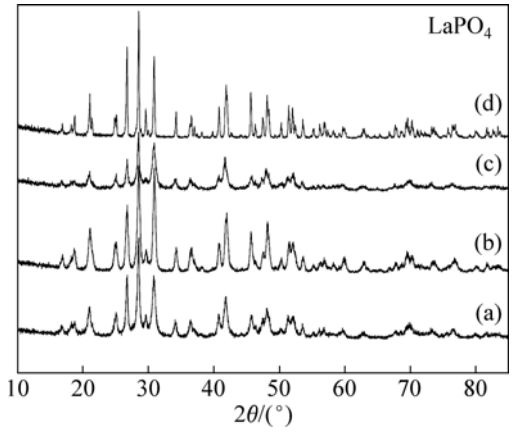

Fig.3 XRD patterns of $LaPO_4$-based nanoparticles after substituting La^{3+} by various contents of Eu^{3+}: (a) $Eu_{0.01}La_{0.99}PO_4$; (b) $Eu_{0.05}La_{0.95}PO_4$; (c) $Eu_{0.10}La_{0.90}PO_4$; (d) $LaPO_4$

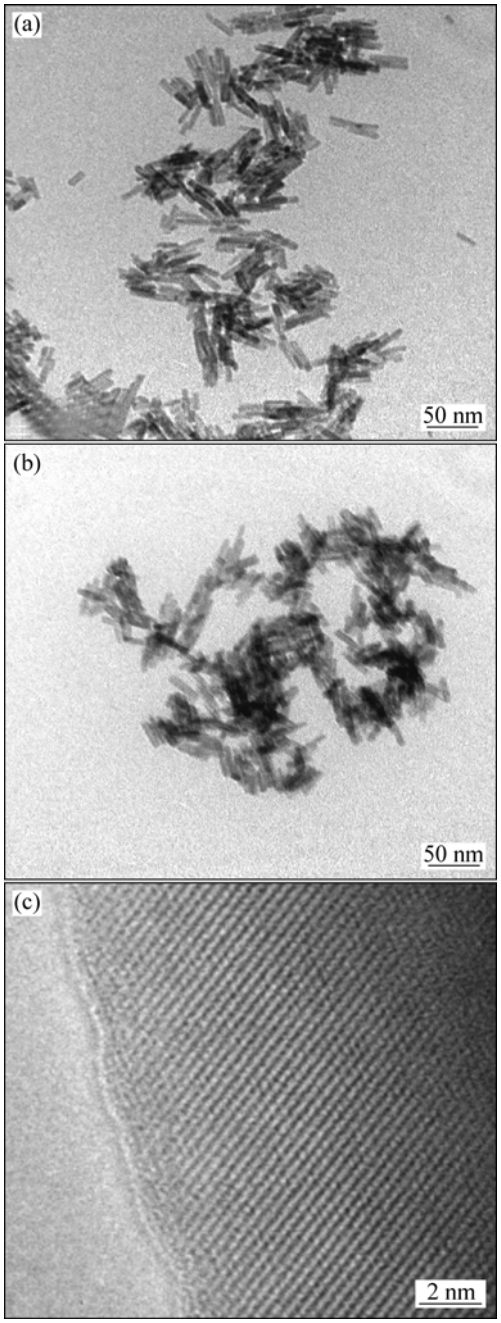

Fig.4 TEM images of as-prepared $Eu_{0.05}La_{0.95}PO_4$ (a), $LaPO_4$ (b) and HRTEM image of $Eu_{0.05}La_{0.95}PO_4$ (c)

3.4 Photoluminescence characterization

The excitation and emission spectra of the nanoscale $Eu_{0.05}La_{0.95}PO_4$ by sol-gel method are presented in Fig.5. Excitation spectrum of the sample is

demonstrated in the left part of Fig.5. The broad band centered at 260 nm is attributed to the charge-transfer band (CTB) between Eu^{3+} and the surrounding oxygen anions[21−23]. There exist five emitting bands which can be seen in the right part of Fig.5. The emission spectrum of the $Eu_{0.05}La_{0.95}PO_4$ mainly locates in the orange-red spectral area (from 550 to 720 nm). The emission located at 540−560 nm can be attributed to the $^5D_0$ -$^7F_0$ transition, while emissions at 585−600 nm, 610−625 nm, 650−660 nm and 680−710 nm correspond to the $^5D_0$ -$^7F_1$ transition, $^5D_0$ -$^7F_2$ transition, $^5D_0$ -$^7F_3$ transition and $^5D_0$ -$^7F_4$ transition, respectively[21−23]. The splitting and intensity pattern of the emission lines demonstrate that the europium has been successfully doped in the sample[24]. The orange-red emission lines at around 595 nm originating from the magnetic dipole transition $^5D_0$ -$^7F_1$ are the dominant bands for the as-synthesized $Eu_{0.05}La_{0.95}PO_4$ nanocrystals.

Physical techniques such as laser ablation have been used to elaborate thin films of Y_2O_3:Eu and YVO_4:Eu phosphors, but they are often difficult to control for complex oxide matrices or doping compositions. Sol-gel routes at relatively high temperature (800−1 000 ℃) have also been largely developed, leading to polycrystalline thin oxide films. The sol-gel process enables a fine control of chemical and physical properties of the matrix in which the nanophosphors are dispersed, and is thus an easy way to obtain transparent and luminescent thin films by spin or dip-coating[25]. Because of these properties, the photoluminescence of nanophosphors synthesized by sol-gel method could be upgraded lagerly though the result is not shown here.

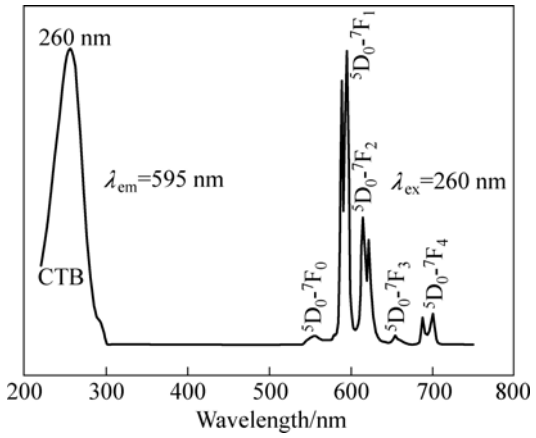

Fig.5 Excitation and emission spectra of $Eu_{0.05}La_{0.95}PO_4$ nanophosphors obtained at 800 ℃

Emission spectra for comparison of different Eu^{3+} doping contents are shown in Fig.6. We can easily conclude that the optimized content of Eu^{3+} is found to be around 5%. The PL intensity is highly depended on activator content. Generally speaking, the brightness tends to increase with increasing activator content. However, the luminescence begins to decrease because pairing or aggregation of activator atoms at high content leads to efficient resonant energy transfer between Eu^{3+} ions and a fraction of energy migration to distant killers or quenchers followed by the appearance of quenching behavior[20, 26]. The concentration quenching behavior of the samples can be evidently observed in Fig.6.

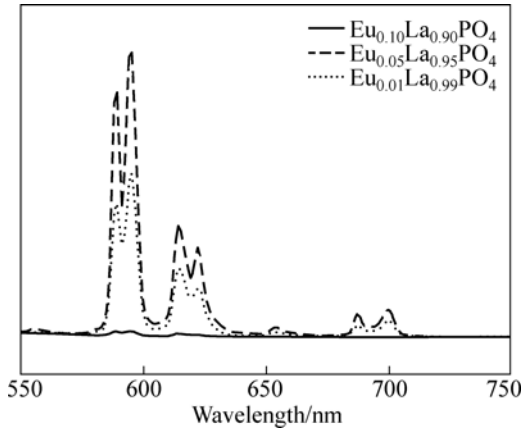

Fig.6 Evolution of emission spectra of $Eu_xLa_{1.0-x}PO_4$ nanophosphors with varying Eu^{3+} doping content

Fig.7 shows the emission spectra of the samples prepared by sol-gel method at different temperatures. It is clear that higher calcination temperature is favorable for brightness of the photoluminescence. The fluorescent materials would quench because of the presence of impure NO_3^- and OH^- ions[27], and high temperature can effectively reduce these quenching centers. There is also another reason that the crystal structure of the sample obtained at higher temperature is reasonably ordered. However, the emission intensity becomes saturated when the temperature is raised above the critical point (1 000 ℃) in these samples.

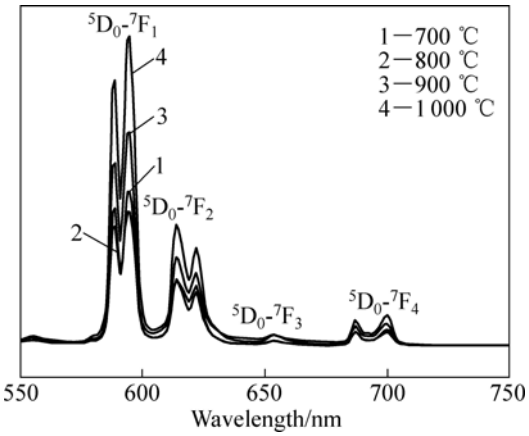

Fig.7 Emission spectra of $Eu_{0.05}La_{0.95}PO_4$ nanophosphors synthesized at different temperatures

4 Conclusions

1) $LaPO_4$:Eu phosphors are successfully synthesized through sol-gel method at moderate temperature (800 ℃).

2) The prepared $LaPO_4$ crystallizes in a single-phase, monoclinic structure with a rod shape, approximately 50 nm in length. A high fraction of europium ions could be effectively doped into the crystal lattice of the monoclinic $LaPO_4$ through the same method.

3) The PL characterization demonstrates that the $Eu_{0.05}La_{0.95}PO_4$ nanophosphor shows the most intense emission, and the higher temperature tends to improve the emission intensity. The sol-gel process can upgrade the photoluminescence properties lagerly. Therefore, the $LaPO_4$:Eu phosphors can be easily applied in various types of lamp and display due to its morphologies and good PL performance. In this regard, our target product is a very promising phosphor. Moreover, the synthesis methods are simple with low-cost, and also be readily extended to other rare earth phosphates.

References

[1] LETANT S E, VAN BUUREN T W, TERMINELLO L J. Nanochannel arrays on silicon platforms by electrochemistry [J]. Nano Letters, 2004, 4(9): 1705−1707.

[2] WANG Xun, ZHUANG Jing, PENG Qing, LI Ya-dong. A general strategy for nanocrystal synthesis [J]. Nature, 2005, 437(7055): 121−124.

[3] GAO Pu-xian, DING Yong, MAI Wen-jie, HUGHES W L, LAO Chang-shi, WANG Zhong-lin. Conversion of zinc oxide nanobelts into superlattice-structured nanohelices [J]. Science, 2005, 309(5741): 1700−1704.

[4] BUDDHUDU S, KAM C H, NG S L, LAM Y L, OOI B S, ZHOU Y, WONG K S, RAMBABU U. Green color luminescence in Tb^{3+}: (La, Ln)PO_4 (Ln=Gd or Y) photonic materials [J]. Materials Science and Engineering B, 2000, 72(1): 27−30.

[5] COLOMER M T, GALLINI S, JURADO J R. Synthesis and characterisation of a green NiO/La(Sr)PO_4-delta cermet anode for phosphate based solid oxide fuel cells [J]. Journal of the European Ceramic Society, 2007, 27(13/15): 4237−4240.

[6] NEDELEC J M, MANSUY C, MAHIOU R. Sol-gel derived YPO_4 and $LuPO_4$ phosphors, a spectroscopic study [J]. Journal of Molecular Structure, 2003, 651: 165−170.

[7] RAJESH K, SHAJESH P, SEIDEL O, MUKUNDAN P, WARRIER K G K. A facile sol-gel strategy for the synthesis of rod-shaped, nanocrystalline, high-surface- area lanthanum phosphate powders and nanocoatings [J]. Advanced Functional Materials, 2007, 17(10): 1682−1690.

[8] GALLINI S, JURADO J R, COLOMER M T. Synthesis and characterization of monazite-type Sr: $LaPO_4$ prepared through coprecipitation [J]. Journal of the European Ceramic Society, 2005, 25(12): 2003−2007.

[9] GUO Yan, WOZNICKI P, BARKATT A. Sol-gel synthesis of microcrystalline rare earth orthophosphates [J]. Journal of Materials Research, 1996, 11(3): 639−649.

[10] FELDMANN C. Polyol-mediated synthesis of nanoscale functional materials [J]. Advanced Functional Materials, 2003, 13(2): 101−107.

[11] BROWN S S, IM H J, RONDINONE A J, DAI S. Facile, alternative synthesis of lanthanum phosphate nanocrystals by ultrasonication [J]. Journal of Colloid and Interface Science, 2005, 292(1): 127−132.

[12] FUJISHIRO Y, ITO H, SATO T, OKUWAKI A. Synthesis of monodispersed $LaPO_4$ particles using the hydrothermal reaction of an $La(edta)^-$ chelate precursor and phosphate ions [J]. Journal of Alloys and Compounds, 1997, 252(1): 103−109.

[13] YOSHIMURA M, SUDA H, OKAMOTO K, IOKU K. Hydrothermal synthesis of needle-like apatite crystal [J]. Nihon Kagaaku Kaishi, 1991, 10: 1402−1407.

[14] FERHI M, HORCHANI-NAIFER K, FERID M. Hydrothermal synthesis and photoluminescence of the monophosphate $LaPO_4$:Eu(5%) [J]. Journal of Luminescence, 2008, 128(11): 1777−1782.

[15] DIAZ-GUILLEN J A, FUENTES A F, GALLINI S, COLOMER M T. A rapid method to obtain nanometric particles of rhabdophane $LaPO_4{\cdot}nH_2O$ center dot nH_2O by mechanical milling [J]. Journal of Alloys and Compounds, 2007, 427: 87−93.

[16] GIAUME D, BUISSETTE V, LAHLIL K, GACOIN T, BOILOT J P, CASANOVA D, BEAUREPAIKE E, SAUVIAT M P, ALEXANDROU A. Emission properties and applications of nanostructured luminescent oxide nanoparticles [J]. Progress in Solid State Chemistry, 2005, 33(2/4): 99−106.

[17] FANG Yue-ping, XU An-wu, SONG Rui-qi, ZHANG Hua-xin, YOU Li-ping, YU J C, LIU Hua-qin. Systematic synthesis and characterization of single-crystal lanthanide orthophosphate nanowires [J]. Journal of the American Chemical Society, 2003, 125(51): 16025−16034.

[18] CAO Min-hua, HU Chang-wen, WU Qing-yin, GUO Cai-xin, QI Yan-juan, WANG En-bo. Controlled synthesis of $LaPO_4$ and $CePO_4$ nanorods/nanowires [J]. Nanotechnology, 2005, 16(2): 282−286.

[19] WANG Ying, TANG Zhi-yong, NICHOLAS A K. Bioapplication of nanosemiconductors [J]. Materials Today, 2005, 8(5): 20−31.

[20] LI Wei, LEE Joonho. Microwave-assisted sol-gel synthesis and photoluminescence characterization of $LaPO_4$:Eu^{3+}, Li^+ nanophosphors [J]. Journal of Physical Chemistry C, 2008, 112(31): 11679−11684.

[21] PATRA C R, ALEXANDRA G, PATRA S, JACOB D S, GEDANKEN A, LANDAU A, GOFER Y. Microwave approach for the synthesis of rhabdophane-type lanthanide orthophosphate(Ln=La, Ce, Nd, Sm, Eu, Gd and Tb) nanorods under solvothermal conditions [J]. New Journal of Chemistry, 2005, 29(5): 733−739.

[22] YI S S, BAE J S, MOON B K, JEONG J H, PARK J C, KIM I W. Enhanced luminescence of pulsed-laser-deposited Y_2O_3:Eu^{3+} thin-film phosphors by Li doping [J]. Applied Physics Letters, 2002, 81(18): 3344−3346.

[23] SCHMECHEL R, KENNEDY M, SEGGERN H V, WINKLER H, KOLBE M, FISCHER R A, LI X M, BENKER A, WINTERER M, HAHN H. Luminescence properties of nanocrystalline Y_2O_3:Eu^{3+} in different host materials [J]. Journal of Applied Physics, 2001, 89(3): 1679−1686.

[24] YAN Ruo-xue, SUN Xiao-ming, WANG Xun, PENG Qing, LI Ya-dong. Crystal structures, anisotropic growth, and optical properties: Controlled synthesis of lanthanide orthophosphate one-dimensional nanomaterials [J]. Chemistry A European Journal, 2005, 11(7): 2183−2195.

[25] BUISSETTE V, GIAUME D, GACOIN T, BOILOT J P. Aqueous routes to lanthanide-doped oxide nanophosphors [J]. Journal of Materials Chemistry, 2006, 6(16): 529−539.

[26] HUANG Hai, XU Guo-qin, CHIN Wee-shong, GAN Leong-ming, CHEW Chwee-har. Synthesis and characterization of Eu:Y_2O_3 nanoparticles [J]. Nanotechnology, 2002, 13(3): 318−323.

[27] HONG G Y, JEON B S, YOO Y K, YOO J S. Photoluminescence characteristics of spherical Y_2O_3:Eu phosphors by aerosol pyrolysis [J]. Journal of the Electrochemical Society, 2001, 148(11): H161−H166.

(Edited by YANG Bing)